Radiometal Conjugate

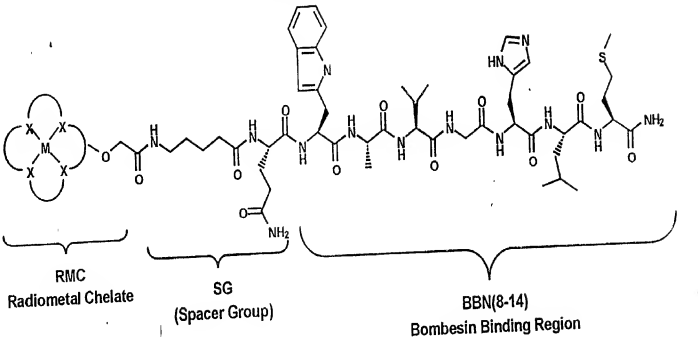

Radiometal conjugate of a BBN analogue that hashigh affinity for GRP receptors.

RMC=Radiometal chelate, where M=^{99m}Tc, $^{186/188}$Re, ^{105}Rh and X=chelating atoms.

SG=Spacer group or linker that covalently attaches the chelate to the N-terminal end of the BBN binding region (BBN_{BR})

Figure 1

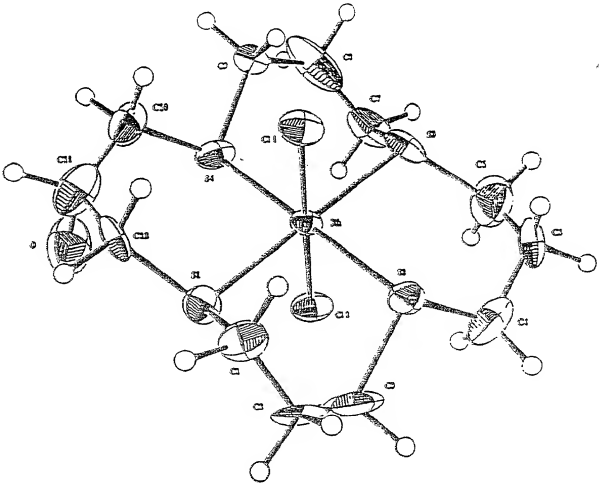

ORTEP Drawing of $\{Rh[16]aneS_4\text{-}oiCl_2\}^+$

Figure 2

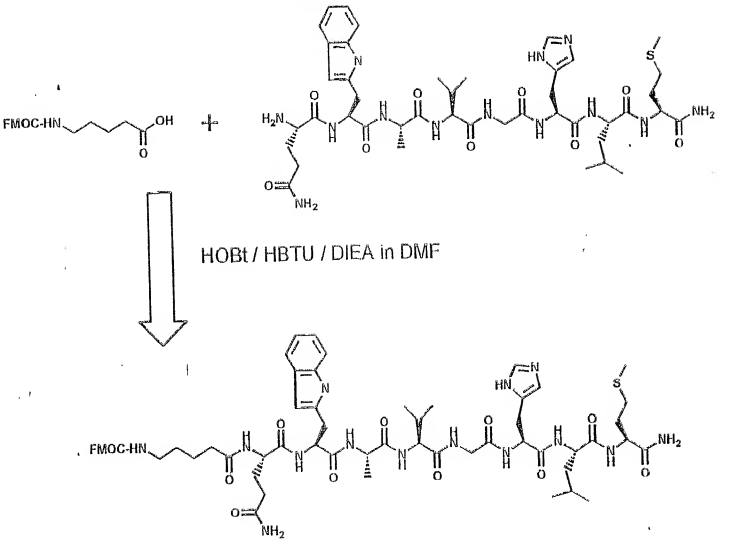

Figure 3

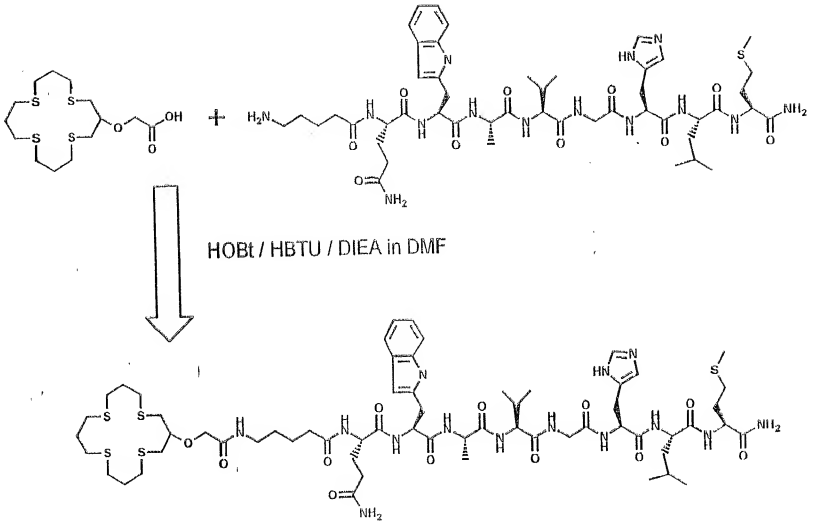

Figure 4

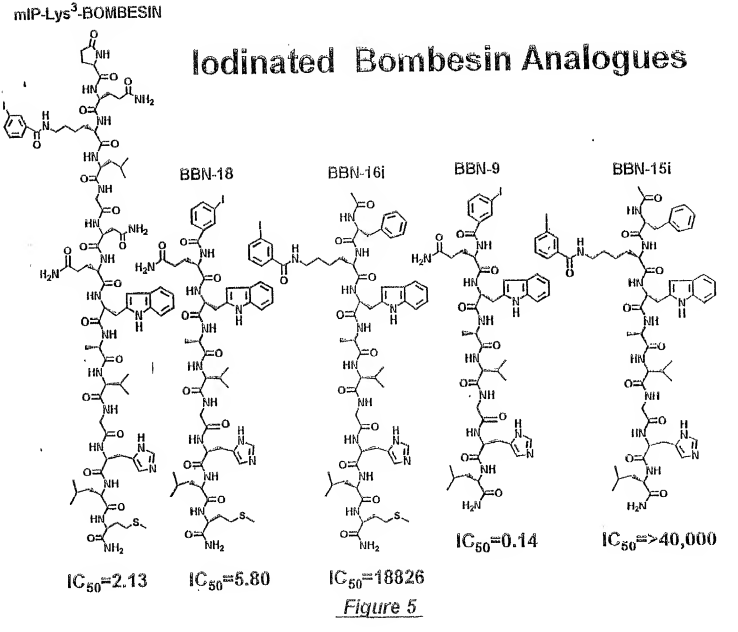

Figure 5

Tethered Bombesin Analogues

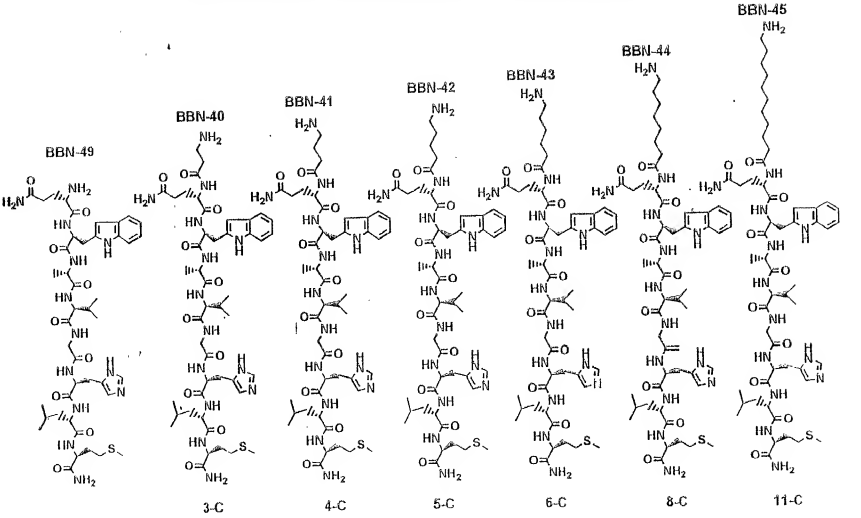

Figure 6

[16]aneS$_4$ Bombesin Analogues

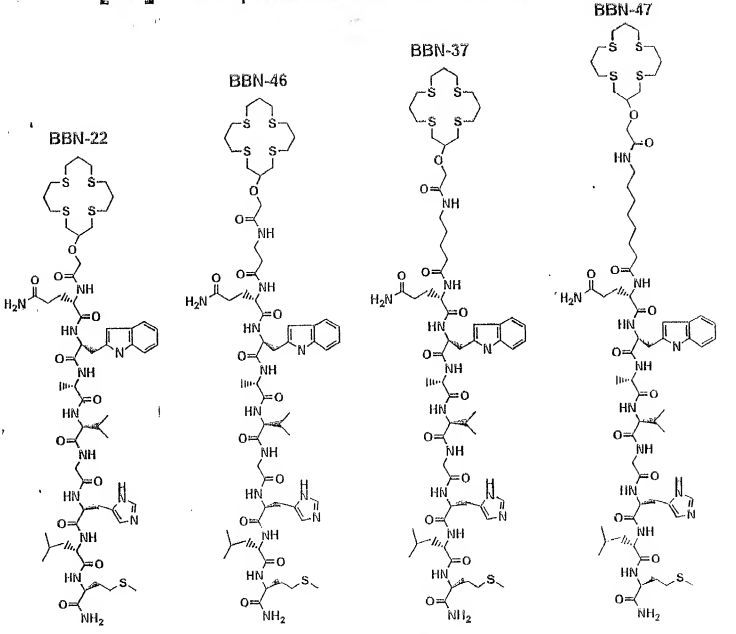

Figure 7

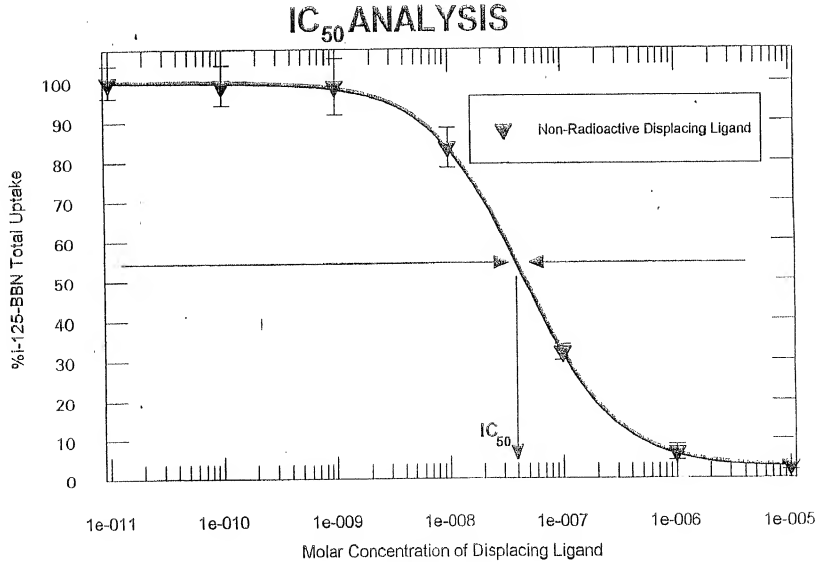

Figure 8

Rhodium-[16]aneS$_4$ Bombesin Analogues

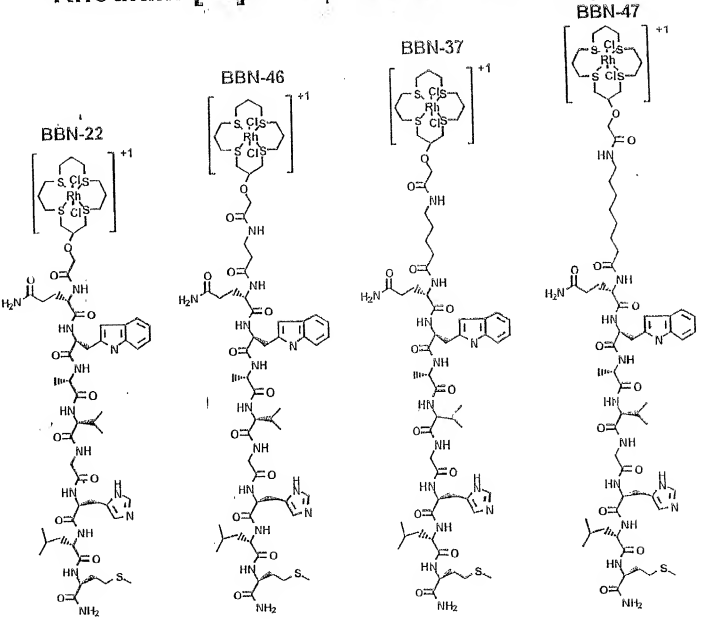

Figure 9

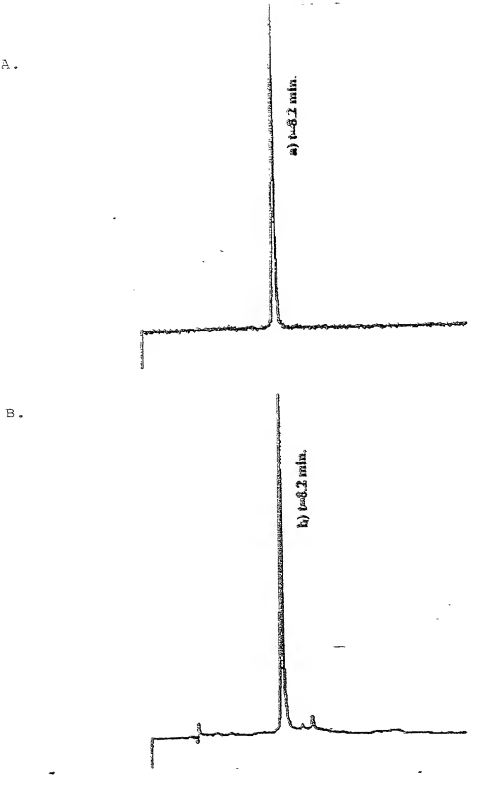

HPLC Chromatogram of Rhodium-BBN-37
Top: $^{105}RhCl_2$-BBN-37
Bottom: $RhCl_2$-BBN-37

Figure 10

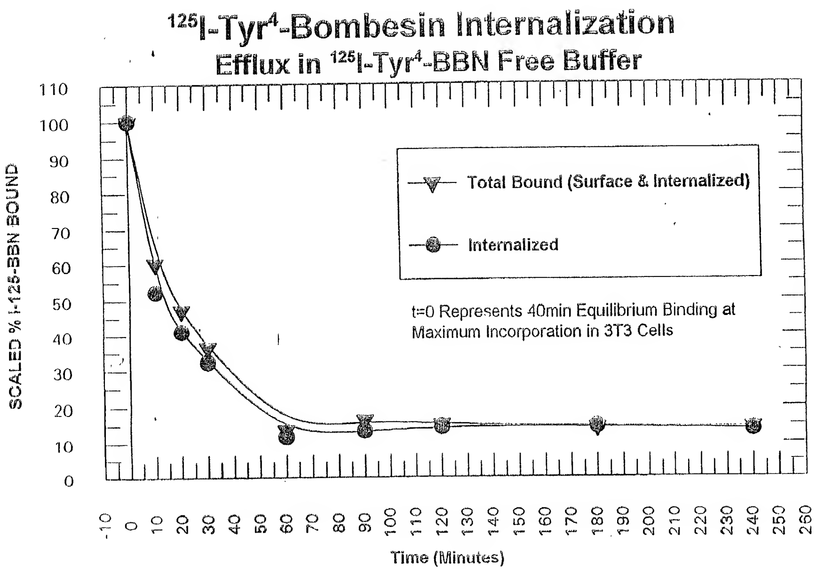
^{125}I-Tyr^4-Bombesin Internalization
Efflux in ^{125}I-Tyr^4-BBN Free Buffer
Total Bound (Surface & Internalized)
Internalized
t=0 Represents 40min Equilibrium Binding at
Maximum Incorporation in 3T3 Cells
SCALED % I-125-BBN BOUND
110
100
90
80
70
60
50
40
30
20
10
0
-10
0
10
20
30
40
50
60
70
80
90
100
110
120
130
140
150
160
170
180
190
200
210
220
230
240
250
260
Time (Minutes)

Figure 11

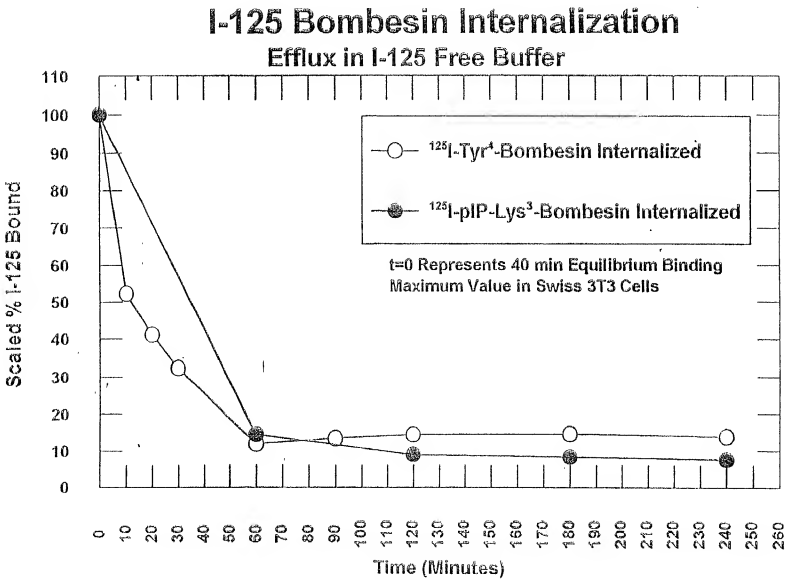

Figure 12

Efflux of ^{105}Rh-BBN-37 in Swiss 3T3 Cells

(Normalized Data)

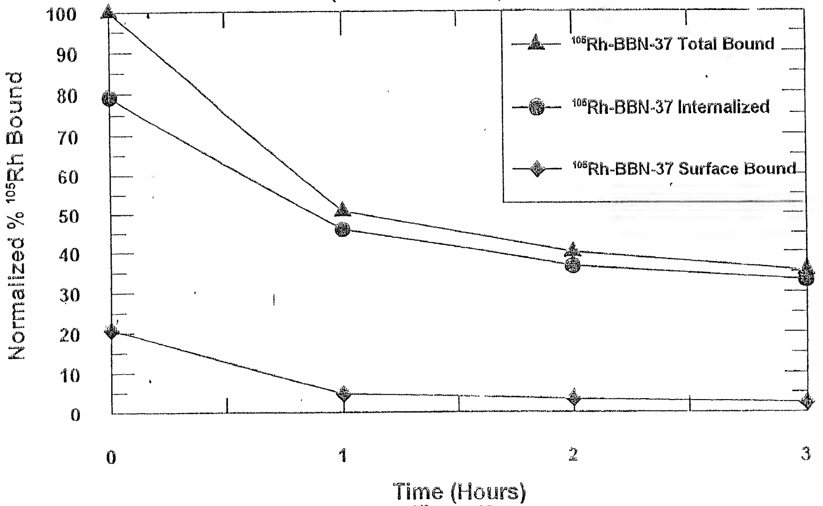

Figure 13

^{105}Rhodium Bombesin Analogues

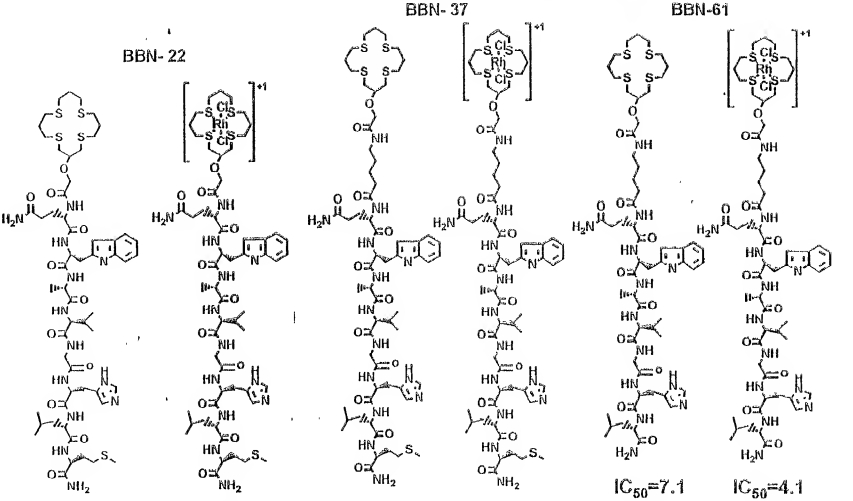

Figure 14

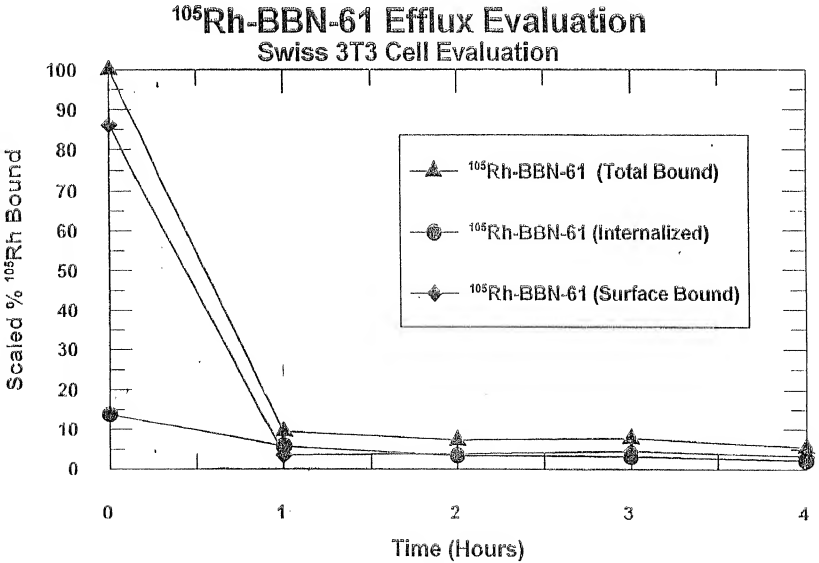
105Rh-BBN-61 Efflux Evaluation
Swiss 3T3 Cell Evaluation
Scaled % 105Rh Bound
100
90
80
70
60
50
40
30
20
10
0
0
1
2
3
4
Time (Hours)
105Rh-BBN-61 (Total Bound)
105Rh-BBN-61 (Internalized)
105Rh-BBN-61 (Surface Bound)

Figure 15

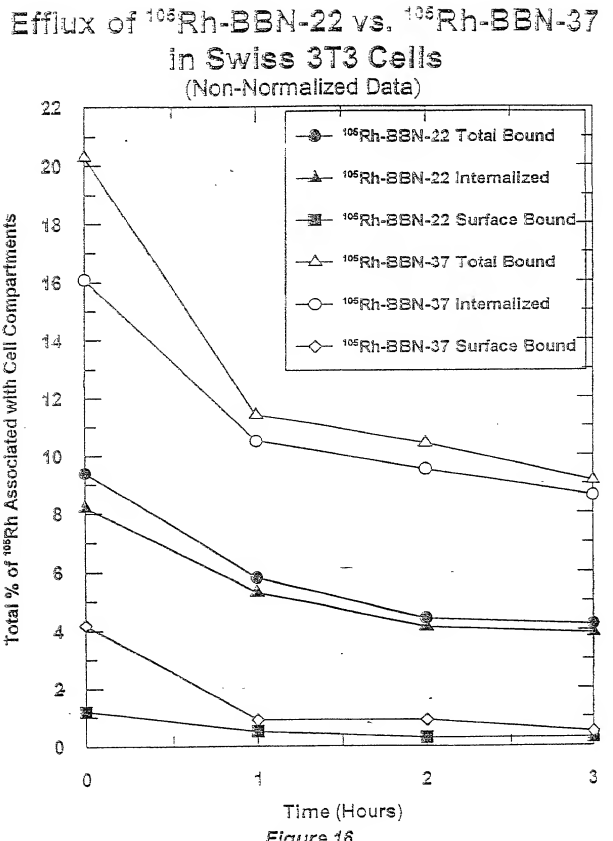
Efflux of 105Rh-BBN-22 vs. 105Rh-BBN-37
in Swiss 3T3 Cells
(Non-Normalized Data)
Total % of 105Rh Associated with Cell Compartments
Time (Hours)
105Rh-BBN-22 Total Bound
105Rh-BBN-22 Internalized
105Rh-BBN-22 Surface Bound
105Rh-BBN-37 Total Bound
105Rh-BBN-37 Internalized
105Rh-BBN-37 Surface Bound
0
2
4
6
8
10
12
14
16
18
20
22
0
1
2
3

Figure 16

Pancreatic CA Cell Binding

A.

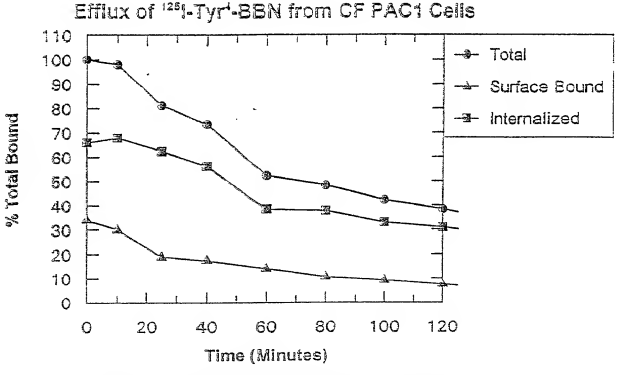

B.

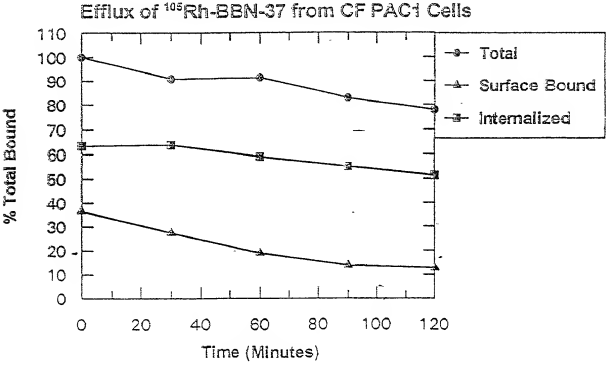

Figure 17

Prostate CA Cell Binding

A.

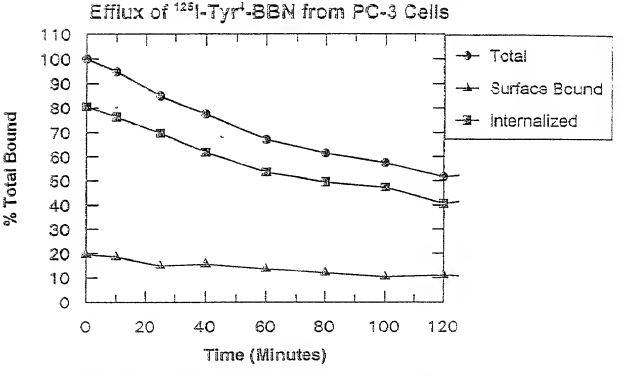

B.

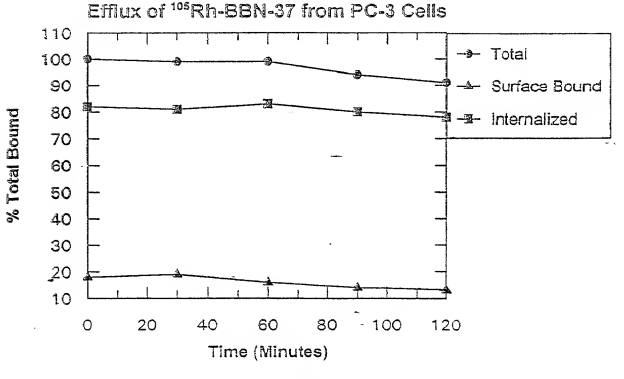

Figure 18

[16]aneS$_4$ Bombesin Analogues

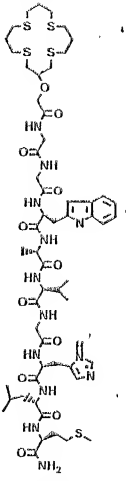

BBN-96

IC_{50} (nM)

Swiss 3T3	18.4 ± 4.5
PC - 3	8.8 ± 1.8
CF PAC - 1	39.5 ± 10.7

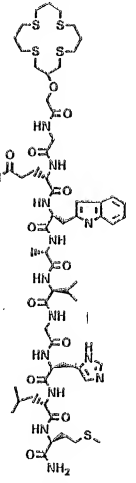

BBN-99

IC_{50} (nM)

	6.0 ± 0.5
	3.3 ± 1.9
	4.8 ± 0.8

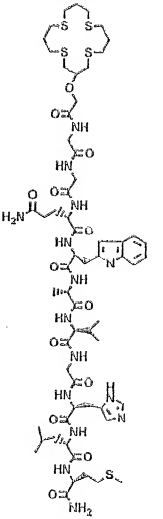

BBN-98

IC_{50}(nM)

	3.3 ± 0.2
	4.3 ± 2.2
	6.1 ± 3.3

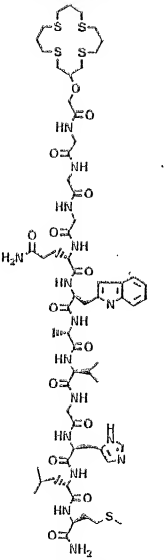

BBN-97

IC_{50}(nM)

	38.0 ± 11.7
	6.9 ± 2.8
	14.2 ± 6.8

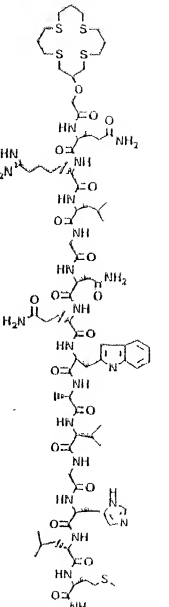

BBN-101

IC_{50}(nM)

	1.2 ± 0.7
	2.1 ± 0.5
	2.4 ± 0.9

FIGURE 19

Rhodium-[16]aneS$_4$ Bombesin Analogues

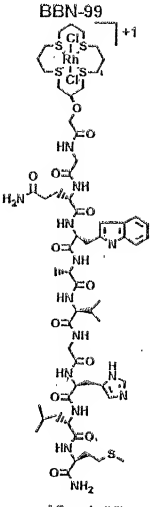

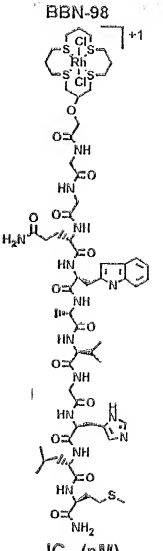

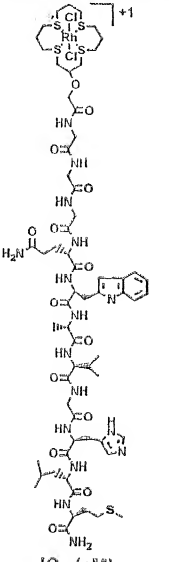

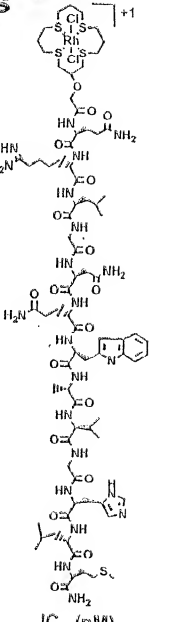

	IC_{50} (nM)	IC_{50}(nM)	IC_{50}(nM)	IC_{50}(nM)
Swiss 3T3	8.24 ± 0.67	2.64 ± 0.76	9.30 ± 1.55	5.42 ± 2.11
PC - 3	4.97 ± 0.60	1.21 ± 0.19	5.29 ± 092	2.32 ± 1.52
CF PAC - 1	4.64 ± 0.81	1.32 ± 0.12	3.70 ± 1.89	0.73 ± 0.83

FIGURE 20

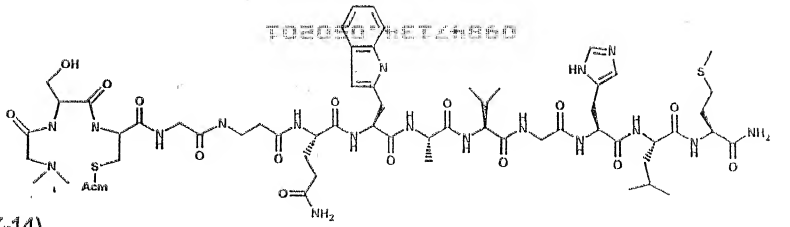

RP414-3C-BBN(7-14)

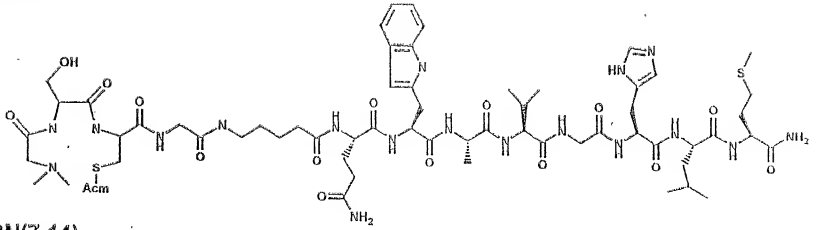

RP414-5C-BBN(7-14)

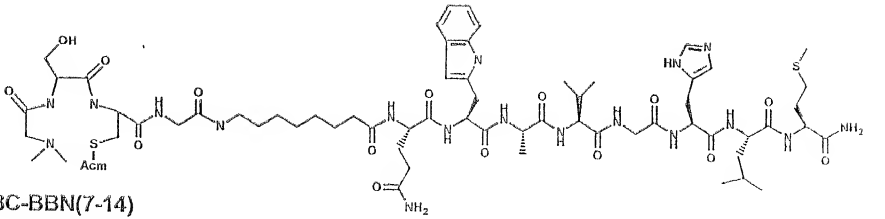

RP414-8C-BBN(7-14)

FIGURE 21

^{99m}Tc-BBN-122

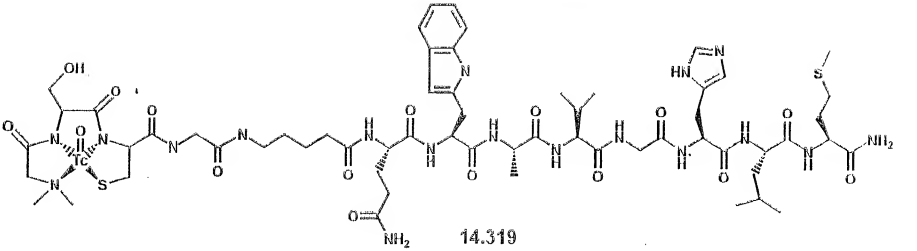

HPLC Gradient Elution Program

Flow 1.5 ml/min
Solvent A = H_2O with 0.1% TFA
Solvent B = CH_3CN with 0.1% TFA

Time(min)	%A/%B
0	95/5
25	30/70
30	95/5

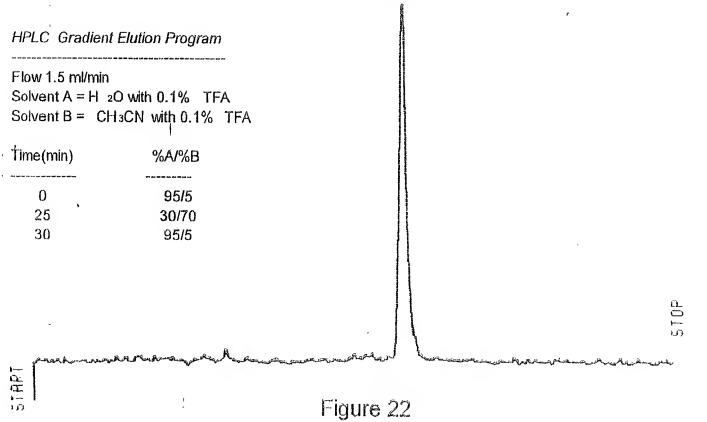

Figure 22

^{99m}Tc-BBN-122 Uptake in Human Prostate Cancer Cells

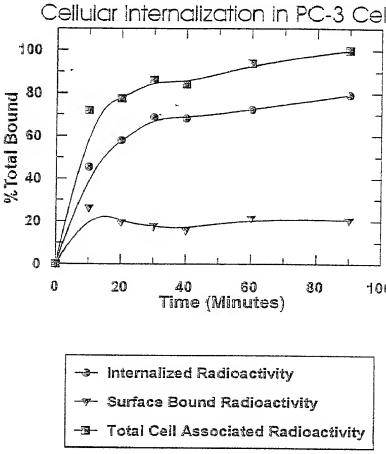

Figure 23

^{99m}Tc-BBN-122 Internalization in Human Pancreatic Cancer Cells

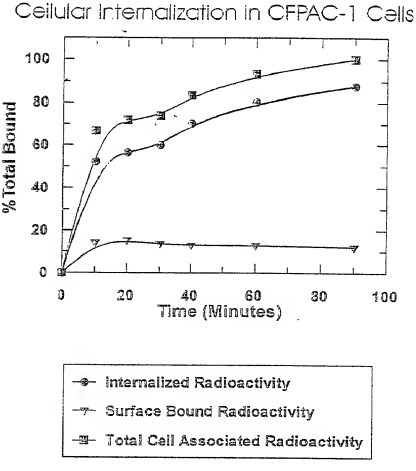

Figure 24

^{99m}Tc-BBN-122 Retention in Human Prostate Cancer Cells

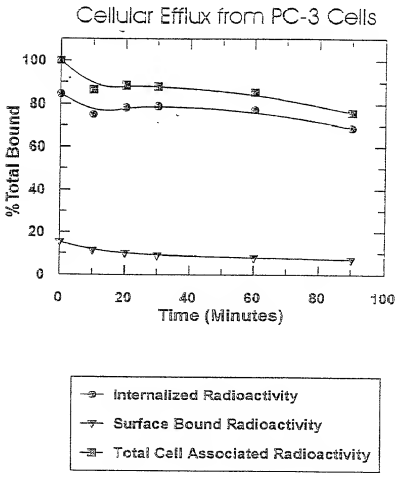

Figure 25

^{99m}Tc-BBN-122 Retention in Human Pancreatic Cancer Cells

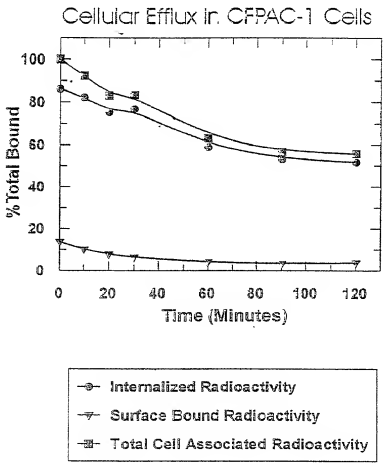

Figure 26

DOTA-BBN[7-14]NH_2 analogues.

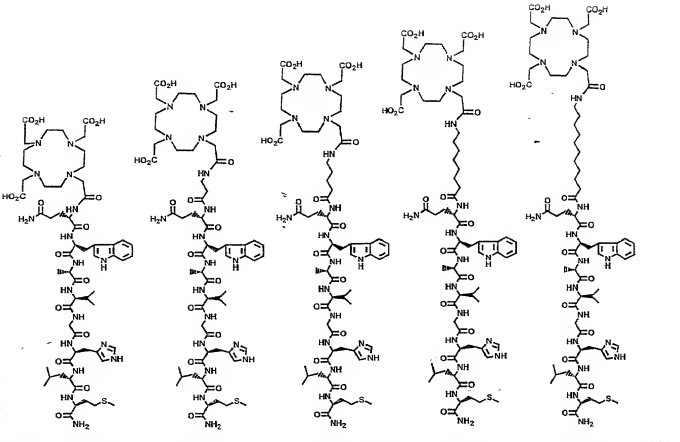

DOTA-0-BBN(7-14)NH_2 DOTA-βAla-BBN(7-14)NH_2 DOTA-5Ava-BBN(7-14)NH_2 DOTA-8Aoc-BBN(7-14)NH_2 DOTA-11Aun-BBN(7-14)NH_2

FIGURE 27

HPLC chromatograms of (a) DOTA-BBN[7-14]NH_2 (λ = 280 nm) (b) In-DOTA-BBN[7-14]NH_2 (λ =280 nm) and (c) ^{111}In-DOTA-BBN[7-14]NH_2 (radiometric).

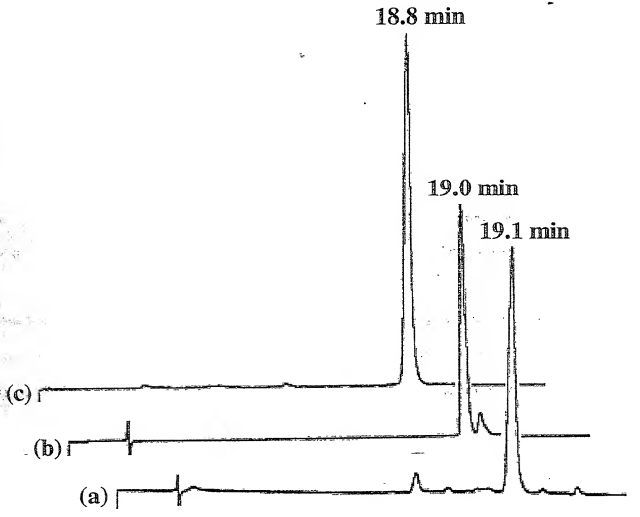

FIGURE 28

Competitive binding assay of In-DOTA-8-Aoc-BBN[7-14]NH_2 vs. ^{125}I-Tyr^4-BBN in PC-3 cells.

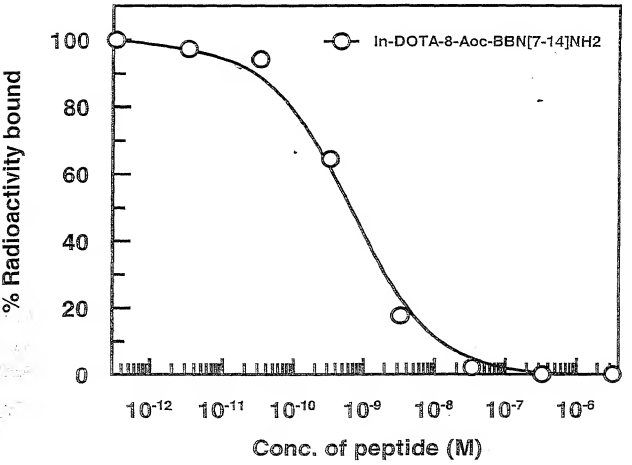

FIGURE 29

Internalization of ^{111}In-DOTA-8-Aoc-BBN[7-14]NH_2 in PC-3 cells.

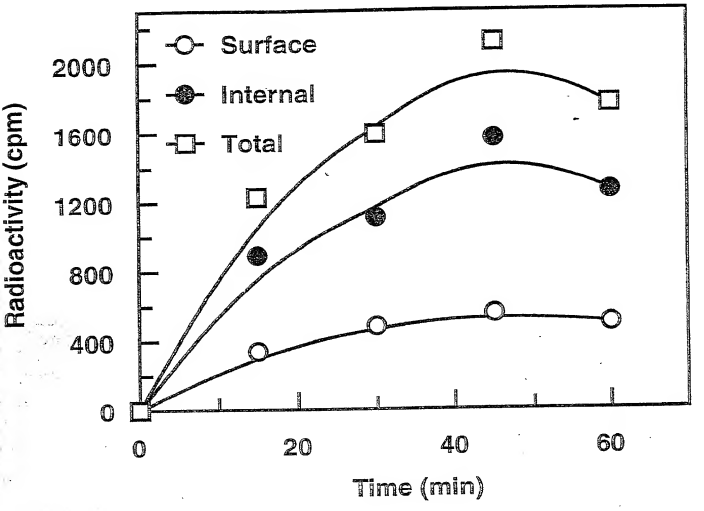

FIGURE 30

Efflux of ^{111}In-DOTA-8-Aoc-BBN[7-14]NH_2 in PC-3 cells.

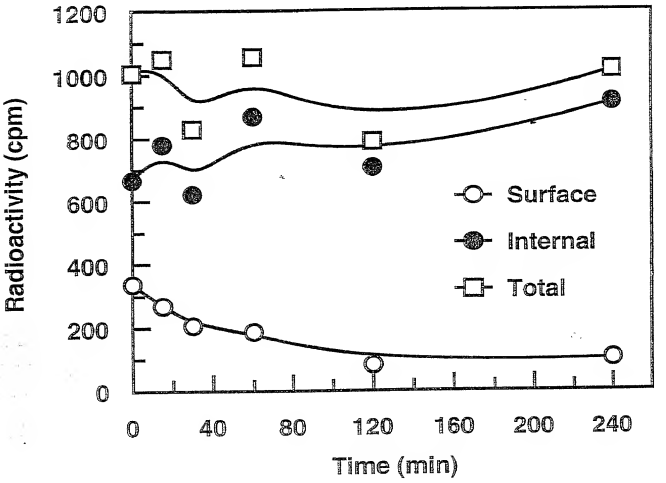

FIGURE 31

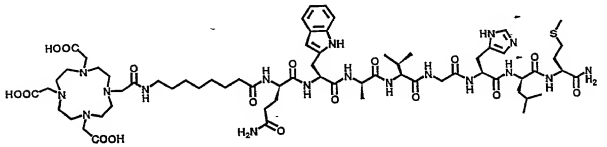

Figure 32